to Ammonium Perchlorate," *Eighth Symposium (International) on Combustion*, Williams and Wilkins, Baltimore, Md., 1962, pp. 678–689.

[14] von Kármán, T., "The Present Status of the Theory of Laminar Flame Propagation," *Sixth Symposium (International) on Combustion*, Reinhold, New York, 1957, pp. 1–11.

[15] Penner, S. S., *Chemistry Problems in Jet Propulsion*, Pergamon Press, Los Angeles, 1957, p. 246.

[16] Beckstead, M. W. and Culick, F. E. C., "A Comparison of Analysis and Experiment for Solid Propellant Combustion Instability," to be published in *AIAA Journal*, 1971.

[17] Burke, S. P. and Schumann, T. E. W., "Diffusion Flames," *Industrial and Engineering Chemistry*, Vol. 20, 1928, p. 998; also *First and Second Symposium on Combustion*, The Combustion Institute, Pittsburgh, Pa., 1965, pp. 2–11.

[18] Williams, F. A., *Combustion Theory*, Addison-Wesley, 1965, pp. 37–45.

[19] Pellett, G. L. and Cofer, G. L., III, "High-Temperature Decomposition of Ammonium Perchlorate Using CO_2 Laser-Mass Spectrometry," AIAA Paper 69-143, New York, 1969.

[20] Pellett, G. L. and Saunders, A. R., "Heterogeneous Decomposition of Ammonium Perchlorate-Catalyst Mixtures Using Pulsed Laser Mass Spectrometry," AIAA Paper No. 68-149, New York, 1968.

[21] Hightower, J. D. and Price, E. W., "Combustion of Ammonium Perchlorate," *Eleventh Symposium (International) on Combustion*, The Combustion Institute, Pittsburgh, Pa., 1967, pp. 1373–1380.

[22] Beckstead, M. W. and Hightower, J. D., "Surface Temperature of Deflagrating Ammonium Perchlorate Crystals," *AIAA Journal*, Vol. 5, No. 10, Oct. 1967, pp. 1785–1790.

[23] Waesche, R. H. W. and Wenograd, S., "Calculation of Solid Propellant Burning Rates from Condensed-Phase Decomposition Kinetics," AIAA Paper No. 69-145, New York, 1969.

[24] Bastress, E. K., "Modification of the Burning Rates of Ammonium Perchlorate Solid Propellants by Particle Size Control," Ph.D. thesis, 1961, Princeton Univ., Princeton, N. J.

[25] Hansen, J. G. and McAlevy, R. F., III, "Energetics and Chemical Kinetics of Polystyrene Surface Degradation in Inert and Chemically Reactive Environments," *AIAA Journal*, Vol. 4, No. 5, May 1966, pp. 841–848.

[26] Anderson, W. H. et al., "A Model Describing Combustion of Solid Composite Propellants Containing Ammonium Nitrate," *Combustion and Flame*, Vol. 3, 1959, pp. 301–318.

[27] Combourieu, J., et al., "Ammonium Perchlorate Combustion Analogue: Ammonia-Chlorine Dioxide Flames," *AIAA Journal*, Vol. 8, No. 3, March 1970, pp. 594–597.

[28] Powling, J., "Experiments Relating to the Combustion of AP-Based Propellants," *11th International Combustion Symposium*, The Combustion Institute, Pittsburgh, Pa., 1967, pp. 447–456.

[29] Coates, R. L., "Linear Pyrolysis Rate Measurements of Propellant Constituents," *AIAA Journal*, Vol. 3, No. 7, July 1965, pp. 1257–1261.

[30] Cohen, N. S., unpublished data obtained on Contract F04611-69-C-0072, Feb. 1970, Lockheed Propulsion Co., Redlands, Calif.

DECEMBER 1970 AIAA JOURNAL VOL. 8, NO. 12

Calibration and Use of Electrostatic Probes for Hypersonic Wake Studies

I. P. French,* R. A. Hayami,† T. E. Arnold,* and M. Steinberg*
AC Electronics—Defense Research Laboratories, Santa Barbara, Calif.

and

J. P. Appleton‡ and A. A. Sonin§
Massachusetts Institute of Technology, Cambridge, Mass.

An experimental shock-tube program was undertaken in order to calibrate spherical and cylindrical electrostatic probes that may be used to make point ion density measurements in continuum flowing plasmas. The empirically derived formula that relates ion density to measured probe current was obtained in terms of appropriate similarity parameters: the Nusselt number for mass transfer of positive ions, dimensionless probe potential, ratio of Debye length to probe radius, and flow Reynolds number. The empirical correlation was used to interpret ion currents collected by a radial array of negatively biased spherical probes, which were positioned so as to intercept the ionized wake of a hypervelocity model in a ballistics range. Integrated ion densities were found to be in good accord with integrated electron densities which were simultaneously measured using microwave methods.

1. Introduction

It has long been recognized that our understanding of the structure and radar-scattering characteristics of the wakes of hypervelocity projectiles might be significantly advanced if time-resolved point measurements of electron density were available in the wakes. Although ballistics ranges do provide an appropriate laboratory environment for making such measurements, and indeed reliable measurements of average electron density as a function of distance behind the projectile have been obtained,[1,2] attempts at measuring local electron density with electrostatic probes have so far been hampered by difficulties with the interpretation of the probe signal.[3,4]

In a recent paper, Sutton[5] proposed a ballistics range experiment that might allow such measurements to be performed with cylindrical collision-free Langmuir probes, held in tension so as to avoid the problem of probe bending. To operate the probe in the collision-free regime, and at the same time have a turbulent wake, requires relatively large ballistics models and low environmental pressures. (Sutton's calculations were based on the theoretically computed wake conditions behind a 6.8 cm diam sphere traveling at 4.72 km sec^{-1} in an ambient pressure of 10 torr.) Unfortunately, the bal-

Received October 13, 1969; revision received March 30, 1970. This work was supported by ARPA and monitored by SAMSO, under Contract F04701-69-C-0125.

* Staff Scientist.
† Staff Engineer. Member AIAA.
‡ Associate Professor, Mechanical Engineering Department.
§ Associate Professor, Mechanical Engineering Department. Member AIAA.

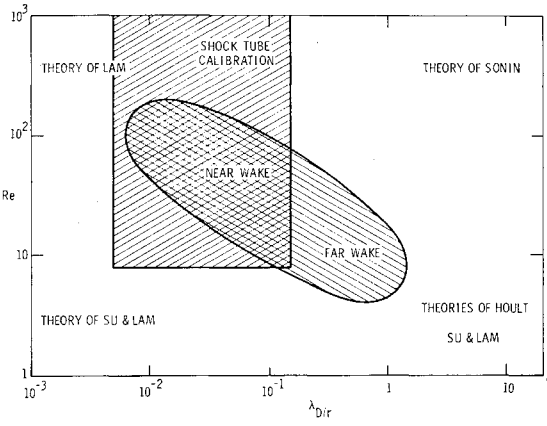

Fig. 1 Range of probe *Re* and λ_D/r covered in a typical wake and also in the present calibration; also shown are limits of available theories.

listics range experiments carried out to date at the AC-DRL facility have been conducted with smaller models, typically spheres that range in diameter from 0.5 cm to 2.5 cm, and at pressures greater than 10 torr.

There are a variety of reasons which lead to the choice of a particular set of conditions for operation of a ballistics range. These depend upon the type of measurement that is to be made; however, one of the most important facts that predicates against large-scale models is the fairly obvious economic one that the cost of the ballistics range facility and its operation increase at a greater than linear rate with increasing model size for a typical re-entry speed of about 6 km sec^{-1}. It seemed reasonable, therefore, to examine the possibility of using electrostatic probes that can be operated in the continuum regime, where the mean-free-path is smaller than the characteristic probe size. The obvious advantage to be gained by adopting this approach is that one can continue to use the existing ballistics ranges and their established methods of operation to investigate wake structure over a considerable range of body size (over at least a factor of 5 in scale size).

Clearly, the crucial problem in using continuum electrostatic probes in the range environment is the method of interpreting the probe current measurements. Although a number of theoretical treatments of probe response in continuum flowing plasmas are available (e.g., Lam,[6] Hoult,[7] Sonin,[8] and Su,[9] to mention only a few representative works), the complexity of the situation is such that each analysis is addressed to specific limiting conditions of flow, probe geometry, etc., and a unified theory spanning the wide range of conditions encountered in a ballistics range is not at present available. Consider, for example, a probe about one millimeter in diameter under typical range conditions.[2] Except in the very near wake (less than about a hundred body diameters downstream of the projectile), the flow in the wake is subsonic,[10] and the primary parameters governing the probe response are expected to be the local Reynolds number based on probe diameter *Re*, the ratio of Debye length to probe radius λ_D/r, and the dimensionless probe potential $\phi = eV/kT$. As the probe passes from the near to the far wake, the Reynolds number ranges from about 200 to 4, and the Debye length ratio from about 10^{-2} to 1, as illustrated in Fig. 1. The available theories, on the other hand, are tailored largely for the limiting conditions of either very small or very large λ_D/r and *Re*, as indicated in the figure. (Note that the situation in Fig. 1 is somewhat oversimplified, since the third coordinate of the similarity parameter space ϕ has been omitted.) Another deficiency in the available theories is their inability to deal with charged-particle collection by the downstream side of the probe, where flow separation occurs; and in a turbulent wake it is generally impractical to use probes with collecting surfaces always oriented into the flow.

It is apparent, therefore, that an experimental calibration of probes is required in flow conditions simulating those of the ballistics range. Such a calibration, and its application in an investigation of hypersonic wakes, is presented in this paper. The probe calibration experiments were carried out using a shock tube where the variation of the electron density behind the primary shock could be measured using a focused microwave interferometer.[11] Most experiments reported here were done with spherical probes so as to eliminate the influence of flow direction on probe response. (A calibration of cylindrical probes is reported briefly in the Appendix.) Only ion collection at negative probe potentials was considered, since electron-collecting probes of the size employed in these experiments were found to draw excessive currents and cause local depletion of the plasma. The range of the probe Reynolds number and the ratio of the Debye length to probe radius covered in this calibration is illustrated in Fig. 1.

The probe calibration part of the experiment is discussed in Sec. 2, and its application to measuring mean ion density profiles in the wakes of hypervelocity projectiles is demonstrated in Sec. 3. Although such probes may also be capable of providing quantitative information on the fluctuating components of the ion density, this paper will limit itself to a discussion of the mean ion density.

2. The Shock-Tube Calibration—Spherical Probes

A. Experimental Apparatus

A pressure-driven stainless steel shock tube having an internal diameter of 15 cm was chosen as a means of providing a flowing plasma whose temperature, pressure, and flow velocity in the region behind the primary shock could be accurately calculated from the known initial conditions and measured shock velocity. The details of construction and method of operation of the shock tube have been described elsewhere in the literature[12] and will not be repeated here.

The test gas used was argon, to which small amounts of acetylene and oxygen (1% C_2H_2 and 5% O_2) were added to produce measureable ionization levels behind the shocks at relatively low temperatures via the process of chemi-ionization. Pressure behind the shock (p_2) was varied between 5 and 1200 torr. In these calibration experiments it was not necessary to know the precise reaction kinetics of the chemi-ionization process, since the temporal variation of electron density was measured directly, using a microwave interferometer (see below). However, it is generally believed that the dominant positive ion persisting after the initial reaction zone in lean acetylene flame[13] and shock-tube studies[12] is H_3O^+, which is then removed via a dissociative recombination reaction of the type

$$H_3O^+ + e^- \rightarrow H_2O + H \text{ (or other neutral products)} \quad (1)$$

Since it was necessary to have some reasonably reliable estimate of the diffusion coefficients of the charged species for our method of data reduction, we assumed that H_3O^+ was the dominant positive ion in the plasma decay region behind the shock wave. (Even if other ions such as CHO^+ made significant contributions to the total positive ion density, we do not think that this would constitute a significant error, since it would enter only through the diffusion coefficient, which is inversely proportional to the square root of the mass.) The only negatively charged species present were electrons, since the temperature range of the present experiments (2000°–7000°K) was too high to allow any significant concentration of molecular negative ions such as O^- and O_2^- to be formed.

The experimental arrangement in the test section of the shock tube is illustrated in Fig. 2. The passage of the primary shockwave through the test gas produced a region of

extremely rapid ionization, which was followed by a much slower decay region. Within these regions the electron density was measured with a focused microwave probe,[2,11] and the ion density was monitored with spherical ion probes.

The 70GHz microwave interferometer uses ($f/2$) dielectric lenses to focus the energy into the centrally located box-like section (width 3.8 cm), which samples the axis flow in the shock tube. This achieves high spatial resolution ($\sim$1 cm), a plane wave in the focal region,[14] and very straightforward interpretation of the data in terms of electron density. The electron densities in the tests were in the range of 10^{10} to 3×10^{11} cm^{-3}, and the plasma was therefore always very underdense to 70 GHz. The largest value of electron collision frequency measured (for $p_2 \approx 1000$ torr and $Re \approx 2000$ to 8000) was 2×10^{11} sec^{-1}. This is still well below the operating frequency (4.4×10^{11} rad/sec^{-1}). Since the measured attenuation was always below 5%, the phase change is almost directly proportional to the electron density.[15] Figure 3a shows a typical oscilloscope signal measured behind an incident shock.

The spherical ion probes (0.76-mm and 3.2-mm diam) were mounted on an insulated sting (0.5-mm diam) that protruded about one probe diam in front of the leading edge of a thin wedge-shaped support. This probe assembly was positioned a short distance ahead of the microwave box and sufficiently far off the shock-tube axis that no disturbance from it could influence the flow within the microwave box. Figure 3b shows measured probe currents, displayed on a logarithmic vertical scale, from two probes biased at -15 v and -30 v; the displays shown in Figs. 3a and b were obtained behind an incident shock in the same experimental test. One major division on the vertical scale of Fig. 3b corresponds to approximately a factor of 10 in probe current. To obtain the calibration, the electron density and probe current were measured at their maximum and about 80 μsec behind the shock arrival, giving two sets of I and n_e (and therefore λ_D) for a single probe voltage and flow condition. The microwave trace (Fig. 3a) beyond about 150 μsec exhibits a slow increase in ionization level, which is probably caused by impurity ionization due to boundary layer heating of the "microwave-box" and window; this part of the trace is not used.

B. Similarity Parameters and Correlation of Probe Data

In order to calibrate a probe in conditions that do not precisely duplicate those where it is to be applied, it is necessary to establish the similarity parameters that govern the probe response. These can be found formally by dimensionless analysis. To facilitate this, we make the following observations about the flow conditions in the present context:

1) The flow about the probes was in or near the continuum regime in the ballistics range as well as in the shock tube where the calibration was performed.

2) Although in the hypersonic wake the flow was turbulent (unsteady), the flow over the probes was assumed to be quasi-steady, which would be true if the probe diameter were small compared with a characteristic turbulent eddy size. Steady flow was established in the shock tube.

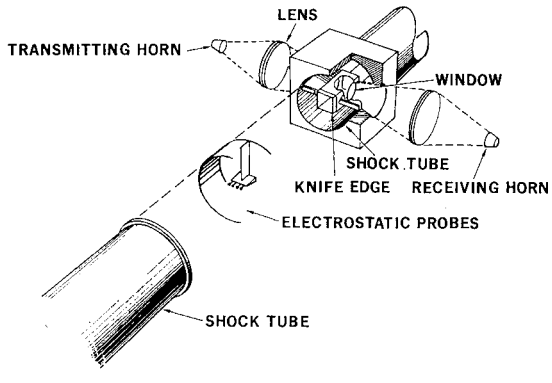

Fig. 2 Electrostatic probes and focused microwave interferometer in shock tube.

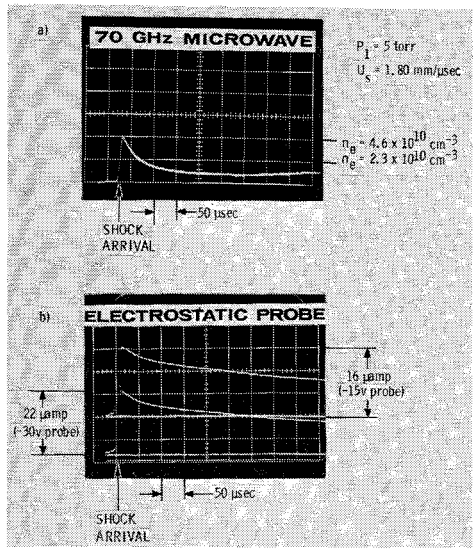

Fig. 3 Response of a) 70GHz microwave interferometer and b) electrostatic probes, to shock-ionized acetylene-oxygen and argon mixture.

3) The flow over the probes was to a good approximation chemically frozen in both test environments. This is almost certainly true in the ballistics range, where the reaction times are considerably longer than the characteristic times associated with the flow about the probes. It was also likely to hold in the shock tube, where the plasma was created by chemi-ionization. It has been proposed[12,16] that chemi-ions and electrons are produced in a short reaction zone behind the primary shock, where there is a large excess of radicals. The electron density that results at the completion of the chemi-ionization reaction is substantially higher than that due to thermal ionization alone. Subsequently, the charged particles are removed by dissociative recombination, which in our shock-tube conditions had a time constant in the neighborhood of 100 μsec, a time that is large compared with the flow time over the probes (<1 μsec). This, together with the fact that significant electron-ion production is unlikely in the weak shock layer itself (since the radical content of the gas behind the primary shock front is low and the temperature increase is slight), makes the assumption of frozen flow over the probes plausible.

4) The gas was weakly ionized.

Under such flow conditions, the current I, drawn by a probe is governed by seven equations: the (frozen) ion and electron conservation equations; Poisson's equation; the conservation equation for mass, momentum, and energy; and the equations of state for the gas. The solution of these equations depends on the following physical quantities: r = probe radius; V = potential of probe with respect to plasma; v_f = flow velocity of gas; ρ,ν = gas density, and kinematic viscosity (local freestream values); T,T_w = gas temperature, and probe wall temperature; n_i,n_e = ion and electron number densities in gas (assumed equal); D_i,D_e = ion and electron diffusion coefficients; m = molecular weight of gas; k,ϵ_0 = Boltzmann's constant, and permittivity of free space; and e = electronic charge.

From dimensional analysis we find that eight independent dimensionless parameters can be formed from the previous quantities: $Re = v_f 2r/\nu$, Reynolds number based on probe diameter; $\lambda_D/r = (1/r)(\epsilon_0 kT/e^2 n_e)^{1/2}$, ratio of Debye length to probe radius; $\phi = eV/kT$, dimensionless probe potential with respect to the ionized gas; $M = v_f/(\gamma RT)^{1/2}$, Mach number ($R$ is gas constant per unit mass); $\gamma = C_p/C_v$ ratio of gas specific heats; $Sc = \nu/D_i$, Schmidt number based on ion diffu-

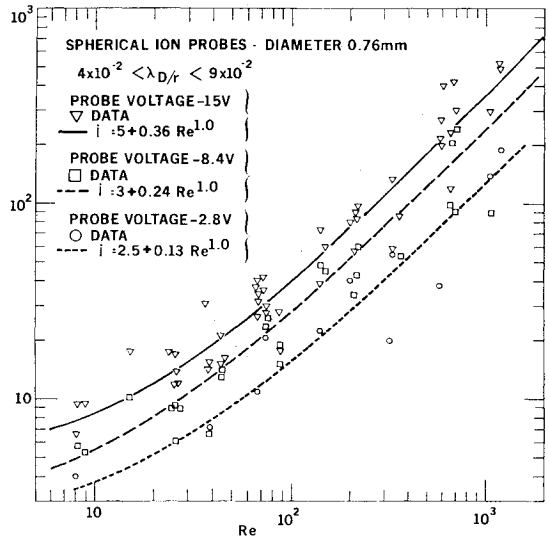

Fig. 4 Shock-tube calibration—i vs Re for three probe voltages: v = −2.8 v (ϕ = −7 to −13), v = −8.4 v (ϕ = −21 to 38), and v = −15 v (ϕ = −38 to −70).

sion coefficient; D_i/D_e = ratio of ion and electron diffusion coefficients; and T_w/T = dimensionless probe wall temperature. It follows that if we define a dimensionless probe current i,

$$i = [Ir/en_iD_i(4\pi r^2)] \tag{2}$$

then this dimensionless current must be a function only of the eight dimensionless parameters listed above, i.e.,

$$i = i(Re, \lambda_D/r, \phi, M, \gamma, Sc, D_i/D_e, T_w/T) \tag{3}$$

We note that i is simply the Nusselt number for mass transfer, often called the Sherwood number, and denoted by Sh, in the chemical literature. The object of a calibration is to measure the dimensionless current i at conditions where the similarity parameters on which it depends have the same values as in the environment where the probe is to be applied, and, hopefully, by covering a sufficiently wide range of the parameters, to infer from the results the functional relationship for i.

In the general case, the function i obviously contains too many variables to yield readily to such an approach. Fortunately, in many circumstances, several of the eight parameters in Eq. (3) are either of secondary importance or essentially invariant, e.g. $Sc \approx 1$ for all gases. Furthermore, if we confine our attention to the collection of ions at relatively high negative probe potentials, the electron diffusion coefficient should not influence the problem significantly ($D_i/D_e \approx 0$). The parameter T_w/T was also assumed to be of secondary importance (its value in these experiments, where the probes remained at essentially room temperature, was small). The insensitivity of i to T_w/T was confirmed by the experiments. This is to be expected in conditions where the boundary layer (i.e., the region in which the influence of the wall temperature could be important) is thinner than the sheath. This was the case in the present experiments, as will be discussed below. Finally, in a low subsonic flow the ion collection would also be insensitive to the Mach number and the specific heat ratio, and the essential parameters would thus be reduced to three in number, i.e.,

$$i = i(Re, \lambda_D/r, \phi) \tag{4}$$

It is the functional form of this relationship that we sought to establish experimentally. It should be pointed out, however, that although over the major portion of the wakes in the ballistics range the flow was indeed subsonic, the calibration experiments were performed in a shock tube where the Mach number M_2, seen by the probes, ranged from 1.1 to 1.4; i.e., it was essentially constant at a low supersonic value. However, based on existing analyses of supersonic blunt probes (e.g., Refs. 8 and 9), it appears reasonable to assume that at such modest Mach numbers, the flow dependence of the ion collection is felt primarily through the Reynolds number rather than the Mach number. The very small range of Mach numbers available in the shock tube (behind the incident shock) prevented a direct check on this point. However, reflected shock measurements[17] did tend to confirm this; and, in addition, a subsequent application of the calibration in the ballistics range (see section 3), where the Mach number ranged to very low subsonic values, yielded good agreement with microwave measurements of electron density. Thus the assumption of Mach number independence appears to be well supported (at least to an accuracy of ±50%).

The calibration procedure in the shock tube was as follows. For given flow conditions ($Re, \lambda_D/r$) and the probe potential ϕ, the probe current I and electron-ion number density n were measured independently, as described in Sec. 2A, and i was calculated. The procedure was repeated for as wide a range of flow conditions as possible, so as to map out the functional form of Eq. (4).

The pressure, temperature, and flow velocity of the test gas were calculated from normal shock-wave relations. The ion-diffusion coefficient was estimated[18] to be equal to $4.8 \times 10^{-3}T^{1.75}/p$ (T in °K and p in torr). A problem that was encountered was the determination of the potential of the plasma, relative to which the probe potential was to be specified. The floating potential of the probes in the shock tube (i.e., the potential where the net current was zero) was established to be within about ½ v of the shock-tube ground. The plasma potential is somewhat positive with respect to the floating potential,[6-8] the difference being of the order kT/e (0.2 to 0.5 v in the shock-tube experiments), the precise value depending on the particular flow conditions. All the voltages referred to in this paper were measured with respect to the shock-tube ground on the assumption that the difference between it and the plasma potential was small compared with the applied voltage.

Some results from the calibration experiments are shown in Figs. 4–7. Our approach was to try to infer from data of this sort an analytic expression for $i(Re, \lambda_D/r, \phi)$ that would satisfactorily correlate all the data. Figure 4 shows typical data of i as function of Re for three values of probe potential, with λ_D/r in the range 4×10^{-2} to 9×10^{-2} for all points. Data of this sort suggested that i may be described by the form

$$i = f(\phi, \lambda_D/r)(a + bRe^{\beta}) \tag{5}$$

where f is an increasing function of ϕ, and a, b, and β may depend on λ_D/r. Figure 5 shows measurements of i as a function of ϕ at a fixed Re and λ_D/r. This and similar data[17] suggest that the potential dependence could be modeled in the

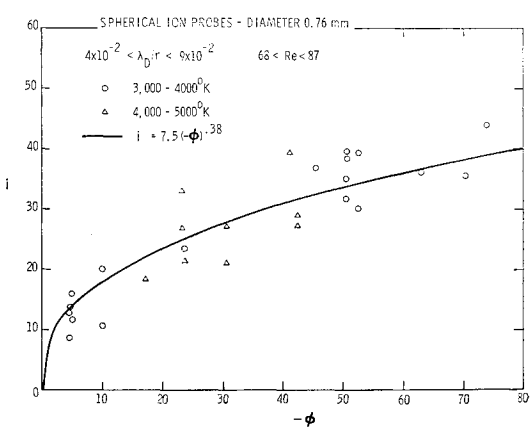

Fig. 5 Dependence of i on probe potential ϕ.

form

$$f(\phi,\lambda_D/r) = (-\phi)^{\alpha(\lambda_D/r)} \quad (6)$$

where α is a function only of λ_D/r. (ϕ,we note, is negative.) α was determined from plots like the one shown in Fig. 5. The results are shown in Fig. 6. The data points are fitted with the analytic relation[17]

$$\alpha = 1/[1 + 0.61\ln(1 + r/\lambda_D)] \quad (7)$$

which was chosen so as to not only fit the data but to extrapolate to the expected theoretical limits $\alpha \to 0$ for $\lambda_D/r \to 0$[19] and $\alpha \to 1$ for $\lambda_D/r \gg 1$[7,8] at the lower Reynolds numbers.

It was found that, to a good approximation, a, b, and β in Eq. (5) could be regarded as independent of λ_D/r and all the results covering the range of parameters: $4 < Re < 10^4$, $10^{-2} < \lambda_D/r < 0.15$, $-10^2 < \phi < -4$, correlated with the relation:

$$i = (-\phi)^{\alpha}(1.2 + 0.09Re^{1.0}) \quad (8)$$

Figure 7 shows Eq. (8) together with all the experimental data plotted in the same form. Clearly, the correlation appears to be reasonably successful. The data fits with an average scatter of about $\pm 50\%$ and shows no systematic deviation from the correlation curve.

C. Discussion and Comparison with Available Theory

Since no theoretical results are available for spherical probes for the conditions of our experiments, a direct comparison of Eq. (8) with theory cannot be made. It is interesting to examine, however, whether Eq. (8) reduces to the theoretically predicted forms when extrapolated to the limits for which explicit solutions are available.

First, consider the limit of a static probe, $Re \to 0$. The theory of Su and Lam[19] for spherical probes yields $i = 2$ for $\lambda_D/r \to 0$, and $i = (-\phi)$ for $\lambda_D/r \gg 1$ (for the latter limit, see also Hoult[7]). Our correlation Eq. (8) reduces to $i = 1.2$ and $i = -1.2\,\phi$, respectively, in these limits. This agreement is quite satisfactory, particularly since our data did not extend to sufficiently low Reynolds numbers to warrant confidence in an extrapolation to $Re \to 0$, and, since in any practical situation the number density in the vicinity of a static probe (and hence the current to it) will be depressed from the ideal value because of diffusion to the probe supports.

An extrapolation of Eq. (8) to high Reynolds numbers, on the other hand, does not yield agreement with the theories available for the limits $\lambda_D/r \to 0$ and $\lambda_D/r \gg 1$. Lam's laminar theory[6] for $Re \gg 1$ predicts $i \sim Re^{1/2}$ in the limit $\lambda_D/r \to 0$, whereas Eq. (8) extrapolates to $i = 0.09\,Re^{1.0}$. For $\lambda_D/r \gg 1$, Sonin's theory[8] predicts $i \sim Re^{1/2}$ for $(-\phi) \ll Re^{1/2}$ and $i \approx (-\phi)$ for $(-\phi) \gg Re^{1/2}$, again in disagreement with Eq. (8).

This disagreement is not surprising. Our correlation equation is an approximate one that was chosen to fit as well as possible all data obtained over the range of conditions of our experiments (Fig. 1). The function i of Eq. (8) is actually a

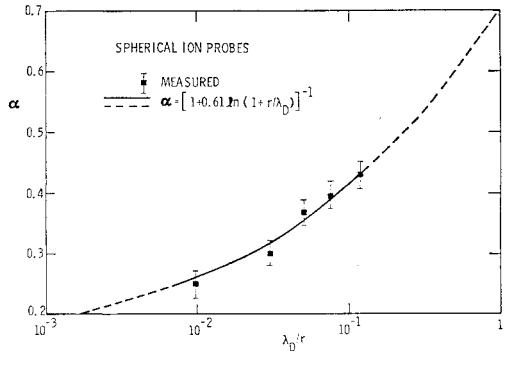

Fig. 6 Shock-tube calibration of α as a function of λ_D/r.

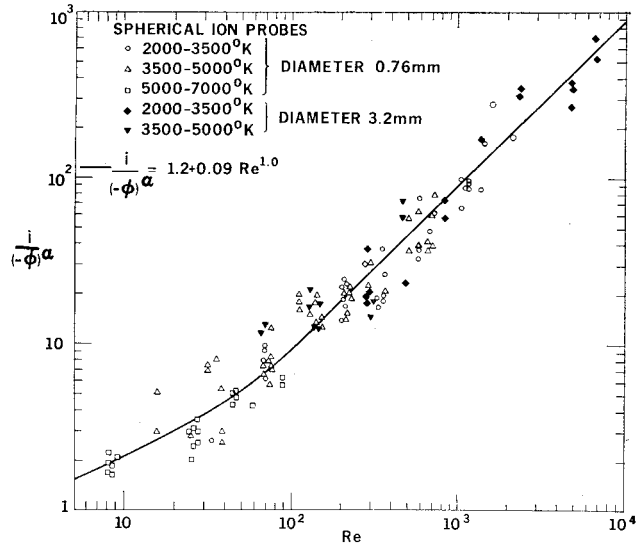

Fig. 7 Correlation of shock tube data in terms of Eq. (8).

very complex one at high Re, as evidenced by the wealth of theories which the electrostatic probe problem has spawned, and there is no reason to expect our approximate correlation to apply outside the region where it was obtained. For example, Lam's theory[6] yields $i \sim Re^{1/2}$ only in the limit where the electrostatic sheath is thin compared to both the boundary-layer thickness and the probe radius; and Sonin's theory[8] is for the case of very large λ_D/r where the probe is unsheathed. In our experiments, on the other hand, the sheath was large compared with the boundary-layer thickness, except at low Re, and comparable, in fact, with the probe radius (but not large compared with r). DeBoer et al.[20] have given an approximate analysis for ion collection by a flat-plate probe under conditions where the sheath is thick compared with the boundary layer. Their result can be written in the form

$$i \sim (\lambda_D/r)^{1/2}(-\phi)^{1/2}Re^{3/4} \quad (9)$$

A quite similar result is obtained if their approach is applied to ion collection in the stagnation point region of a sphere or a cylinder,[17] with the assumption that the sheath is thick compared with the boundary layer but thin compared with the body radius. (The difference resides only in a constant, which has, in any case, been omitted from the equation quoted above.) The above equation does not agree well with the present spherical probe experiments, where the sheath was estimated to be not only thicker than the boundary layer, but often comparable with the probe radius. Numerical computations for flat probes with thick sheaths have also been performed by Dukowicz.[21] In a certain range of λ_D/r and Re, Dukowicz correlates his computed results with a formula which in our notation reads $i \sim (-\phi)^{1/2}Re^{1/2}$. Dukowicz also shows experimental data for slender conical probes which he fits with the relation $i \sim (-\phi)^{0.3}Re^{0.7}$.

A point of interest is that in the limits $Re \gg 1$ and $\lambda_D/r \to 0$, our correlation equation (8) implies that

$$I = 0.9env_f(\pi r^2) \quad (10)$$

i.e., that the collected current is essentially equal to the flux of ions "swept out" of the flow by the cross section of the probe. Noting next that the flow velocity was close to the average thermal speed v_{th} of the ions at our low supersonic Mach numbers, we see that the same equation can be rearranged to yield

$$I \approx (en\bar{v}_{th}/4)(4\pi r^2) \quad (11)$$

One would, indeed, anticipate a relation like Eq. (10) for a probe in a hypersonic, collision-free flow, and a relation such as Eq. (11) for a probe in a stationary, collision-free plasma

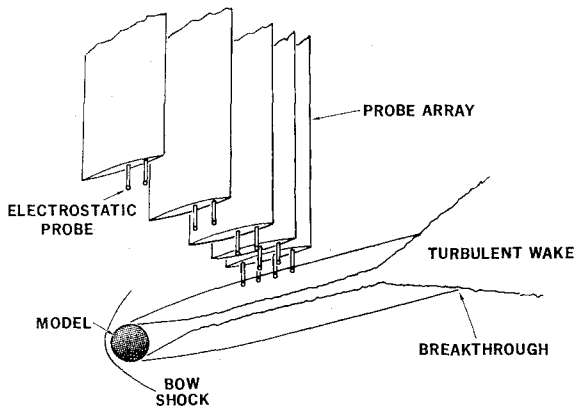

Fig. 8 Electrostatic probes in free-flight range.

That they both happen to be implied simultaneously by an experimental correlation formula obtained at continuum flow conditions (mean free path/probe radius from 10^{-4} to 10^{-1}) at high Re and $M \approx 1$ should not, necessarily, be taken to mean that the mechanism of ion collection in continuum flows is either the "sweeping out" of ions from the flow or their arrival at the probe by simple random, collision-free flux.

Expressions of the type shown in Eqs. (10) and (11) have been used[22,23] to reduce electrostatic probe data in continuum flowing plasmas when $\lambda_D/r \ll 1$. In hypersonic wakes, however, the latter condition is not met and, in addition, v_f is generally much smaller than $\bar{v}_{th}$. The full calibration [Eq. (8)] then has to be used. Our factor $(-\phi)^\alpha$ is, of course, related to the sheath size, which may be thought of as increasing the collection area of the probes.

The following section describes work where the empirical calibration formula, Eq. (8), was used to interpret spherical probe data taken in the wakes of hypersonic projectiles. As we shall see, good agreement was obtained with microwave measurements over several orders of magnitude in electron density (despite, we note, the difference in Mach number in the two environments). This leaves us with some confidence that our calibration technique is successful and accurate to perhaps $\pm 50\%$.

3. Application to Hypersonic Wakes

An array of twelve spherical electrostatic probes was installed in the AC-DRL ballistics range to map electron and ion density distributions behind hypervelocity projectiles (see Fig. 8). The calibration of the previous section was then used to calculate ion density distributions in the wake from the mean current collected by the ion probes. For purposes of computation we set $\nu/D_i = 0.8$ and rearranged Eq. (8) in the form

$$I = (-\phi)^\alpha en(4\pi r^2)(1.2D_i/r + 0.225v_f) \qquad (12)$$

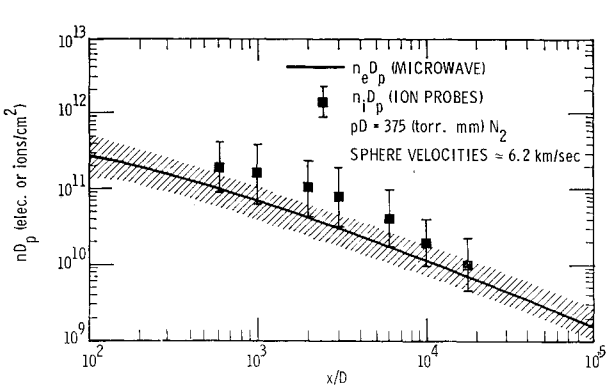

Fig. 9 Comparison of integrated ion density (electrostatic probes) and integrated electron density (microwave probes).

The profiles of temperature and wake velocity used were those calculated by Wen,[24] which are in essential agreement with the measurements made at Canadian Armament Research and Development Establishment (CARDE).[25] The ion density radial profiles so obtained[17,26] were integrated over the wake width to give a quantity we label n_iD_p (D_p may be thought of as an equivalent plasma "diameter"). These values of n_iD_p are compared in Fig. 9 with the integrated electron density n_eD_p as measured with probes and resonators[2,11,27] in nitrogen wakes. The agreement is good considering that the wake is turbulent and our knowledge of even its mean properties (such as v_f and T) is very imperfect.

4. Summary

The present work demonstrates that the continuum electrostatic probe is a useful instrument for making point measurements of charge density in the wakes of hypervelocity projectiles. The difficulty due to the lack of an accurate theory for probe operation in the conditions of a typical ballistics range was overcome by a calibration of spherical, ion-collecting probes in a shock tube. From this calibration, an analytic correlation formula [Eq. (8)] was obtained for the probe current as a function of the appropriate similarity parameters over a wide range of conditions. This empirical correlation equation was used to interpret the readings of probes arranged so as to intersect the wakes of hypersonic projectiles in the ballistics range. Axial and radial profiles of charged particle density were obtained. The results were in good agreement with microwave measurements of integrated electron density.

Appendix: Calibration of Cylindrical Probes

Some results are presented here from a calibration of cylindrical, ion-collecting probes oriented with their axes both parallel and transverse to the flow velocity. The data cover a fairly limited range of the similarity parameters that govern probe response, and do not represent a complete calibration of cylindrical probes. Nevertheless, it has some fundamental interest, and is pertinent to applications in the ballistics range.

The experiments were performed in the shock tube as described in Sec. 2. Two cylindrical probe geometries were employed. The probes aligned with the flow had a radius r of 0.11 mm and length l of 20 mm, while those oriented with their axes perpendicular to the flow had a radius of 0.15 mm and length of 2.0 mm, mounted on an aerodynamic sting and cantilevered forward into the flow. The calibration is again expressed in terms of a dimensionless probe current i defined

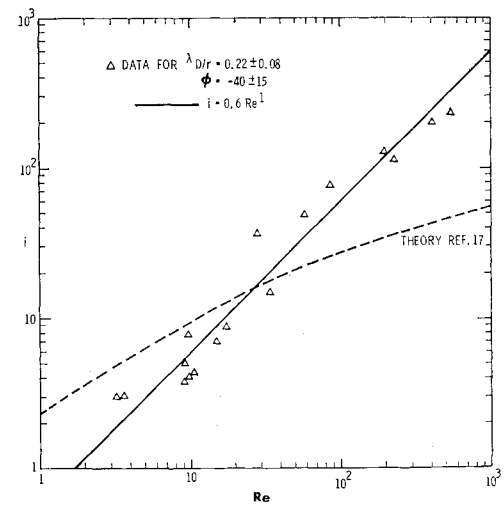

Fig. 10 Calibration of cylindrical probe perpendicular to flow; r = 0.15 mm, l = 2.0 mm, λ_D/r = 0.22 ± 0.08, ϕ = −40 ± 15.

as in Eq. (2) with $(2\pi rl)$ replacing $(4\pi r^2)$. Proceeding as in Sec. 2, it can be shown that for a cylindrical probe the dimensionless current is primarily a function of four dimensionless similarity parameters, Re, λ_D/r, ϕ, and l/r. Re is the Reynolds number based on probe diameter, as in the case of the spherical probes, and the fourth parameter l/r is the probe's aspect ratio. We note that if $l/r \gg 1$, i is expected to be independent of l/r for a probe perpendicular to the flow, but not for a probe aligned with the flow. This is because the boundary layer (and the sheath) scales with r for a perpendicular probe, but with l for an aligned probe.

In our experiments, the Reynolds number was varied over three orders of magnitude from about 1 to 10^3. The dependence of i on λ_D/r and ϕ, however, was explored only qualitatively, since the measurements involved only two values of each of these parameters for each probe orientation. The aspect ratio l/r was kept fixed at 13.3 for the probes perpendicular to the flow and 182 for the aligned probes.

Figures 10 and 11 show some results for the calibration of a probe perpendicular to the flow direction, in the form of a plot of i vs Re. We note that the indicated spread in λ_D/r and ϕ (e.g., $\phi = -40 \pm 15$) does not represent an inaccuracy of measurement, but merely reflects the grouping of experimental data. Each set of data points has been fitted with a simple relationship of the form $i \sim Re^{\beta}$. The data of Fig. 10 can be fitted with an exponent $\beta \approx 1$, just as in the case of spherical probes under similar conditions, whereas for the data of Fig. 11, where the sheath is thinner (in both cases the sheath is of the order of the probe radius), a somewhat smaller exponent $\beta \approx \frac{3}{4}$ gives a better fit. As expected, the smaller sheath size in Fig. 10 results in somewhat lower dimensionless current than in Fig. 11 at the same Reynolds number.

Theoretical solutions for the dimensionless probe current are available or can be derived by means of available techniques only for certain limiting cases. Lam[6] deals with the case of a thin laminar boundary layer in the limit $\lambda_D/r \to 0$ (sheath $\ll$ boundary layer $\ll$ probe size), where the ion collection is controlled by diffusion across the boundary layer and is essentially independent of probe potential. For a cylindrical probe perpendicular to the flow, such an analysis yields $i \sim Re^{1/2}$, while for a cylinder aligned with the flow, one obtains approximately $i \sim (l/r)^{-1/2} Re^{1/2}$.

Our data (Figs. 10 and 11) do not agree with this theory, presumably because in the experiments, the sheath was of the order of the probe radius and thick compared with the boundary layer, in violation of the assumptions in the theory. For example, for the case with $\phi = -40$ and $\lambda_D/r = 0.22$, we estimate that the sheath thickness is about one probe radius

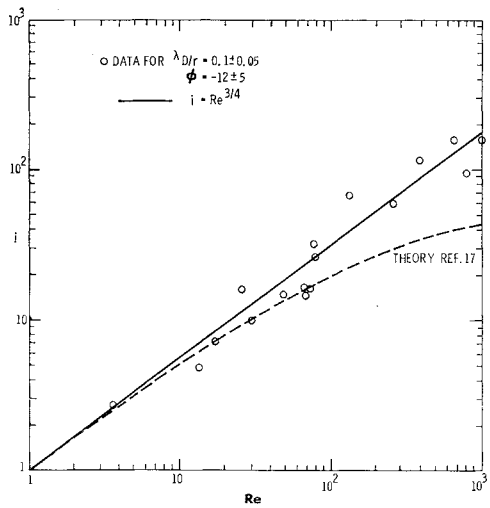

Fig. 11 Calibration of cylindrical probe perpendicular to flow; $r = 0.15$ mm, $l = 2.0$ mm, $\lambda_D/r = 0.1 \pm 0.05$, $\phi = -12 \pm 15$.

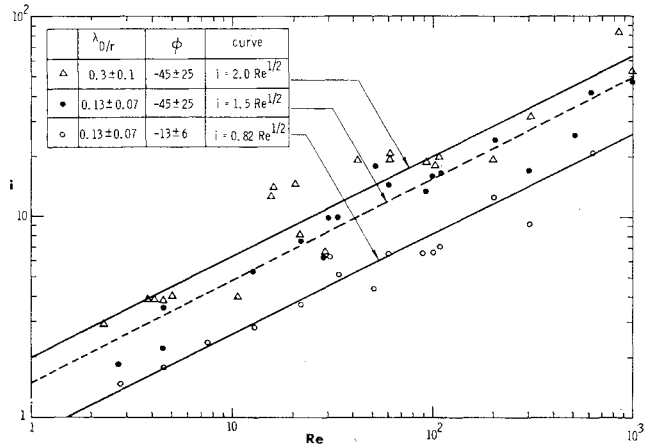

Fig. 12 Calibration of cylindrical probe aligned with flow; probe radius $r = 0.11$ mm, length $l = 20$ mm, $l/r = 182$.

at $Re \sim 10^2$, while for $\phi = -12$ and $\lambda_D/r = 0.1$ (Fig. 11) it is about $\frac{1}{2}$ probe radius. The viscous boundary layer thickness at the same Reynolds number is about 0.15 probe radius.

The results for the aligned probe (Fig. 12) however, do agree better with the thin-sheath boundary layer theory. The $Re^{1/2}$ dependence is clearly there, although there is a significant dependence also on both λ_D/r and ϕ, which would be absent for a sufficiently small sheath. The reason for this better agreement is presumably that the thickness of the boundary layer for a probe aligned with the flow is approximately $(l/r)^{1/2}$ as much as for a perpendicular probe of the same radius in the same flow. Thus, at $Re \approx 10^2$, for example, the boundary layer is a few probe radii in thickness, while typically in Fig. 12 the sheath thickness is about one probe radius. The conditions are thus somewhat closer to those of a diffusion controlled theory, although the sheath is by no means thin enough for the theory to apply accurately.

We note that an approximate theory has been derived by deBoer et al.[20] for a flat-plate probe in conditions where the sheath is thick compared with the boundary layer, but thin compared with the probe dimensions (boundary layer $\ll$ sheath $\ll$ probe size). We have extended their method of solution to current collection in the stagnation region of cylindrical probes oriented perpendicular to the flow, in order to compare with the results of Figs. 10 and 11, where the boundary layer is thinner than the sheath (although the sheath is not small compared with the probe size, which is the other major assumption in this theory). The agreement, however, was quite poor.[17] The theory[17] is shown by the dotted line in Figs. 10 and 11.

In conclusion, then, we have presented here an empirical calibration of cylindrical electrostatic probes in a flowing environment, covering a limited range of the similarity parameters that govern the probe response. No theory is available for the range of conditions covered in our experiments, and we have shown that an optimistic application of some existing theory to our results could incur considerable error.

References

[1] Kornegay, W. M., "Electron Density Decay in Wakes," *AIAA Journal*, Vol. 3, No. 10, Oct. 1965, pp. 1819–1823.

[2] Hayami, R. A. and Primich, R. I., "Wake Electron Density Measurements Behind Hypersonic Spheres and Cones," *AGARD Conference Proceedings, No. 19; Fluid Physics of Hypersonic Wakes*, May 1967, Ft. Collins, Colo.

[3] Herrman, J. et al., "Some Statistical Properties of Turbulent Wakes," *AGARD Conference Proceedings No. 19; Fluid Physics of Hypersonic Wakes*, May 1967, Ft. Collins, Colo.

[4] Heckman, D., Cantin, A., and Kirkpatrick, A., "Electrostatic

Probe Measurements in the Turbulent Wake of Hypersonic Spheres Fired in a Ballistics Range," *AGARD Conference Proceedings, No. 19; Fluid Physics of Hypersonic Wakes*, May 1967, Ft. Collins, Colo.; also *AIAA Journal*, Vol. 5, No. 8, Aug. 1967, pp. 1494–1495.

[5] Sutton, G. W., "Use of Langmuir Probes for Hypersonic Turbulent Wakes," *AIAA Journal*, Vol. 7, No. 2, Feb. 1969, pp. 193–199.

[6] Lam, S. H., "A General Theory for the Flow of Weakly Ionized Gases," *AIAA Journal*, Vol. 2, No. 2, Feb. 1964, pp. 256–262.

[7] Hoult, D. P., "D-Region Probe Theory," *Journal of Geophysical Research*, Vol. 70, No. 13, July 1965, pp. 3183–3187.

[8] Sonin, A. A., "Theory of Ion Collection by a Supersonic Atmospheric Sounding Rocket," *Journal of Geophysical Research*, Vol. 72, No. 17, Sept. 1967, pp. 4547–4557.

[9] Su, C. H., "Compressible Flow Over a Biased Body," *AIAA Journal*, Vol. 3, No. 5, May 1965, pp. 842–848.

[10] Zivanovic, S., Robillard, P. E., and Primich, R. I., "Radar Investigation of the Wakes of Blunt and Slender Hypersonic Velocity Projectiles in the Ballistics Range," *AGARD Conference Proceeding, No. 19; Fluid Physics of Hypersonic Wakes*, May 1967, Fort Collins, Colo.

[11] Primich, R. I. et al., "Two New Techniques for Determination of Transient Plasma Properties," *Proceedings of Seventh International Conference on Phenomena in Ionized Gases*, Vol. III, 1966, pp. 128–130.

[12] Wilson, L. N. and Evans, E. W., "Electron Recombination in Hydrocarbon-Oxygen Reactions Behind Shock Waves," *Journal of Chemical Physics*, Vol. 46, No. 3, Feb. 1967, pp. 859–863.

[13] Calcote, H. F., "Ion and Electron Profiles in Flames," *Proceedings on Ninth Symposium (International) on Combustion*, Academic Press, New York, 1963, pp. 662–637.

[14] Born, M. and Wolf, E., *Principles of Optics*, Pergamon Press, New York, 1959.

[15] Zivanovic, S., Musal, H. M., Jr., and Primich, R. I., "Determination of Plasma Layer Properties from Measured Electromagnetic Transmission Coefficient," *IEEE Transactions on Antennas and Propagation*, Vol. AP-12, No. 5, Sept. 1964, pp. 618–624.

[16] Green, J. A. and Sugden, T. M., "Some Observations on the Mechanism of Ionization in Flames Containing Hydrocarbons," *Proceedings of the Ninth Symposium (International) on Combustion*, Academic Press, New York, 1963, pp. 607–621.

[17] French, I. P. et al., "Calibration and Use of Spherical and Cylindrical Electrostatic Probes for Hypersonic Wake Studies," TR69-12, Dec. 1969, AC Electronics-DRL, Santa Barbara, Calif.

[18] Dalgarno, A., *Diffusion and Mobilities in Atomic and Molecular Processes*, edited by D. R. Bates, Academic Press, New York, 1962, pp. 643–662.

[19] Su, C. H. and Lam, S. H., "Continuum Theory of Spherical Electrostatic Probes," *The Physics of Fluids*, Vol. 6, No. 10, Oct. 1963, pp. 1479–1491.

[20] DeBoer, P. C. T., Johnson, R. A., and Thompson, W. P., "Flat Plate Probe for Measuring Ion Density," AIAA Paper 68-165, New York, 1968; also *The Physics of Fluids*, Vol. 11, No. 4, April 1968, pp. 909–911.

[21] Dukowicz, J. K., "Theory and Calibration of Small Continuum Electron Probes in Ionized Flow," *Record of International Congress on Instrumentation and Aerospace Simulation Facilities*, IEEE Publication 69C 19-AES, May 69, pp. 52–62; see also Rept. RA-2641-7-1, Jan. 1969, Cornell Aeronautical Labs.

[22] Bredfeldt, H. R. et al., "Boundary Layer Ion Density Profiles as Measured by Electrostatic Probes," *AIAA Journal*, Vol. 5, No. 1, Jan. 1967, pp. 91–98.

[23] McLaren, T. I. and Hobson, R. M., "Initial Ionization Rates and Collision Cross Sections in Shock-Heated Argon," *The Physics of Fluids*, Vol. 11, No. 10, Oct. 1968, pp. 2162–2172.

[24] Wen, K. S., Chen, T., and Lieu, B., "Theoretical Study of Hypersonic Sphere Wakes in Air and Comparisons with Experiments, Part I: Turbulent Diffusion," AIAA Paper 68-703, Los Angeles, Calif., 1968.

[25] "Reentry Physics Research Program in Turbulent Wakes," TN 1807/68, CARDE Semiannual Progress Report, June 1968.

[26] French, I. P., Arnold, T. E., and Hayami, R. A., "Ion Distributions in Nitrogen and Air Wakes Behind Hypersonic Spheres," AIAA Paper 70-87, New York, 1970.

[27] Hayami, R. A. and Kelley, K. J., "Open Microwave Resonators for Ionized Wake Measurements," *IEEE Transactions on Aerospace and Electronics Systems*, Vol. AES-2, No. 2, March 1967, pp. 339–348.